38th International Electric Vehicle Symposium and Exhibition (EVS38)
Göteborg, Sweden, June 15-18, 2025

Wallbox Inspection – Evaluating Solar Controlled Charging of EV Charging Equipment

Bernhard Wille-Haussmann[1], Jan Körber[1],
Nico Orth[2], Joseph Bergner[2]
[1]*Fraunhofer Institute for Solar Energy Systems ISE, Heidenhofstrasse 2,*
79110 Freiburg, Germany, bernhard.wille-haussmann@ise.fraunhofer.de
[2]*University of Applied Sciences Berlin, Wilhelminenhofstr. 75 A 12459 Berlin*

Executive Summary

To make electric mobility possible and acceptable on a large scale, it is necessary to integrate electric vehicle (EV) charging infrastructure in residential energy systems. Solar surplus charging, a special case of controlled charging is a popular and promising operating mode of installed systems. Comparison of different home energy management systems (HEMS) in combination with a dedicated EV charging station reveals differences in control quality. Within the research project Wallbox-Inspektion, a test setup and procedures to determine the main criteria for evaluating the quality of solar surplus charging were developed. This contribution explains the tests for standby consumption and control quality of control steps and presents an approach to determine the influence in use case scenarios. Further, different solar charging systems (i.e. charging station, HEMS, energy meter) available on the market are compared and discussed regarding the quality of implemented solar charging strategies.

Keywords: Electric Vehicles, AC & DC Charging technology, Smart charging, V2H & V2G, Energy management

1 Introduction

Since solar energy becomes one of the cheapest way to produce energy, on-side solar charging is one of the most rewarding strategies for residential EV charging [1]. To control EV charging power according to the available solar power owners of residential energy systems need to implement home energy management system (HEMS). The HEMS measures the residual load and controls the EV supply equipment (EVSE) to maximize the share of photovoltaic in the electricity supply. Typically, the charging equipment defines via the pilot signal according to IEC 61851 [2] the maximum charging current of the EV. Field observations and the example plotted in fig. 1 show that the system reaction to a change of the residual load can take up to several minutes. Consequently, this affects self-consumption and self-sufficiency.

To evaluate this effect, this paper introduces a test procedure to measure the quality of solar controlled charging systems for electric vehicles. First, the test setup and the test routines are described. Second, the measurement for four EV charging solutions available on the market will be compared. Finally, the results are discussed, and their importance for the performance of solar charging is classified.

In this paper, results for standby consumption and control quality will be covered. Further, an approach to determine the impact on a use case scenario is presented. It should be emphasized that this is the

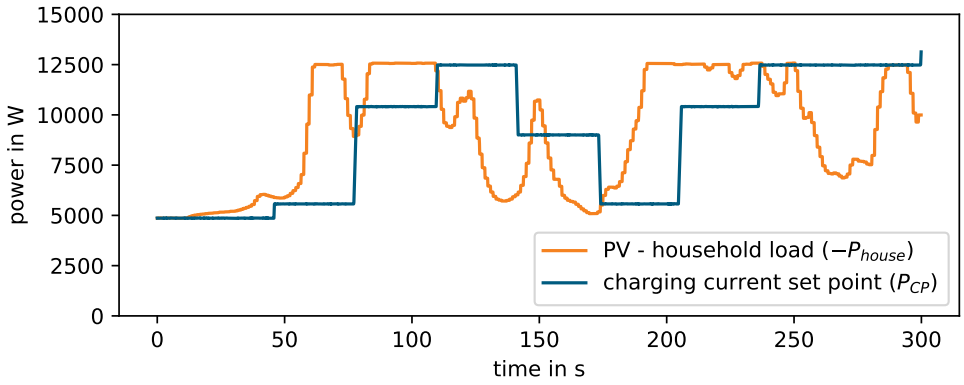

Figure 1: Result of a solar controlled charger following the surplus of PV. The resulting power set point P_{CP} is delayed against the PV surplus $-P_{house}$.

first study on the comparability of solar home charging systems based on comprehensive, standardized laboratory measurements. Furthermore, this article contributes a proposal on a standardized efficiency assessment for EV charging equipment.

2 Test Environment

Since field testing of charging systems is not standardized and different system components are mixed, the results of these trials can hardly be compared. A test environment is therefore set up to measure the solar charging systems consisting of the main components EVSE, HEMS and energy meter, in a setup recommended by the manufacturer.

Within the environment, the surroundings will be emulated in the Power Hardware-in-the-Loop (HIL) at the Digital Grid Lab [3] at Fraunhofer ISE. An graphical representation of the test setup is shown in fig. 2. In addition to power terminals, it shows power flows and communications to the tested system. This includes on the one hand the power measurements M_{net}, M_{EV} and M_{house} with its positive direction marked and on the other hand the IEC 61851 communication. As real power flows are measured, the tested system is connected to the public grid which is tracked by M_{net}. Furthermore, the household is emulated by a bidirectional load emulation of the type Cinergia. The resulting power flow is measured by M_{house}.

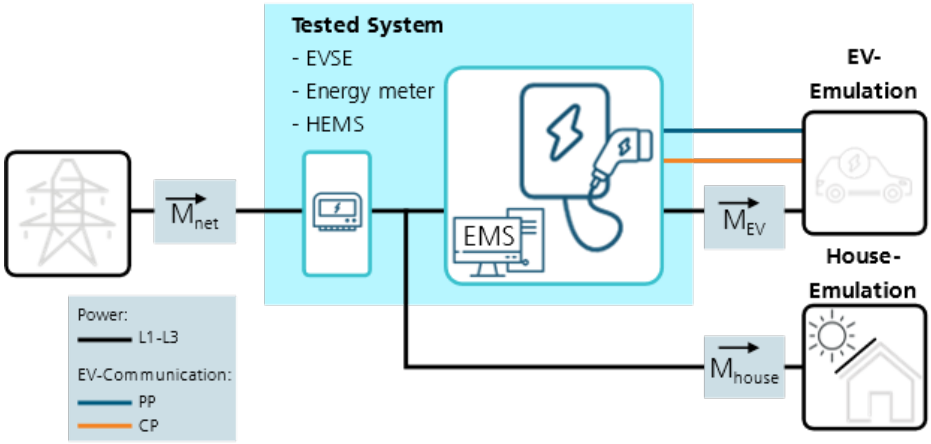

Figure 2: Test environment for evaluating system reactions for solar controlled charging including the emulated grid, EV, and house. Positive measurement directions are marked.

The EV is emulated by a digital twin of an EV called “ev twin” [4, 5]. The “ev twin” is developed by Fraunhofer ISE in the HIL environment typhoon HIL. It emulates the charging process according to IEC 61851 [2] and allows full Power-HIL testing and access to all model parameters. It enables totally reproducible test results, decoupling the charging system test of influences of the EV. Among the model

parameters are the results of the control pilot (CP) signal evaluation, which communicates the maximum allowed current I_{CP} to the EV. Further details see [4] and [6].

3 Test Procedure

The test environment described above allows full testing of EV charging system for private households. In fig. 3 the charging station's power set point P_{CP} follows the residual load reference $-P_{house}$. P_{CP} is derived from maximum allowed current I_{CP} using the voltages at M_{house}, as the charging station communicates current set points. The sequence can be divided into different operational phases, exemplary marked in fig. 3:

- standby (section 3.1)
- control steps (section 3.2)
- switching between one- and three-phase charging
- start and stop charging

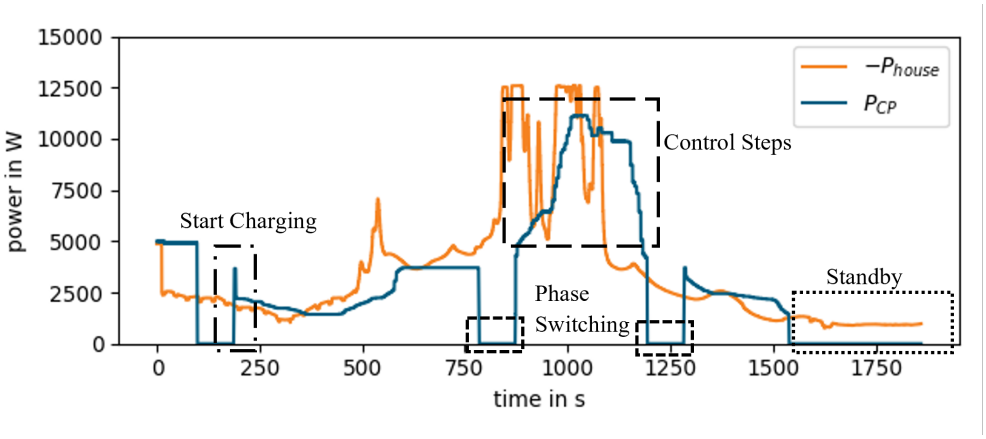

Figure 3: The charging system's power set point P_{CP} (derived from I_{CP}) follows the photovoltaic surplus $-P_{house}$ for 30 min. The section is divided in the operational phases: start charging, switching between one and three phase charging, control steps, and standby.

The operational phases can be investigated and parametrized separately to allow for detailed comparability of different system implementations. For that, dedicated static test procedures are developed within the test framework [7]. This paper describes test procedures that focus on standby consumption and control quality of control steps. Further, an approach to determine performance in an application scenario is presented. It aims at enabling correlation of the parametrization derived in the static tests with performance in the selected application scenario. Detailed setup, further information and test procedures can be found in [7]. In this section the selected test procedures are presented.

3.1 Standby Consumption

As EV supply equipment is operated most of the time in standby state, e.g. with a connected car and waiting for photovoltaic surplus or while waiting for the EV, the standby consumption needs to be observed. According to IEC 61851 [2] three system states are important to investigate:

- A: no EV connected, the EVSE should be in idle mode.
- B: EV connected, no charging requested by EV.
- C: EV connected, charging requested by EV but no surplus energy available.

For both system states the measurements of M_{net} are acquired while the emulated EV and the household consumption are disabled, i.e. $P_{house} = 0$ W and $P_{EV} = 0$ W. In this setup the measured power from the net P_{net} equals the standby power $P_{standby}$. The test procedure is straightforward. First, the environment is set to a state fulfilling the requirement of the above mentioned system states A, B or C. Secondly, after a short settling period, $P_{standby}$ is obtained. Third, there is a waiting time in which either a maximum of 30 minutes is waited or it is determined that the EVSE enters deep standby mode with reduced consumption. In order to get reproduceable results, the test is repeated two times at a minimum.

3.2 Control Quality

In contrast to uncontrolled charging, solar charging has to react to the fluctuating nature of PV surplus and requires a fast and accurate reaction of the HEMS. Hence, the second test evaluates the control quality by the mean of the settling time towards a new maximum charging current set point. Figure 4 illustrates the expected reaction after a trigger through a change in the current I_{house}. Note that the negative current indicates a surplus of on-site generation. Therefore, a decreasing step at I_{house} is followed by an increasing permissible charging current for the EV I_{CP}. It's worth to notice that, as the test setting does not include an assessment of the EV, the maximum allowed charging current by the EVSE via the duty cycle of the CP signal is evaluated.

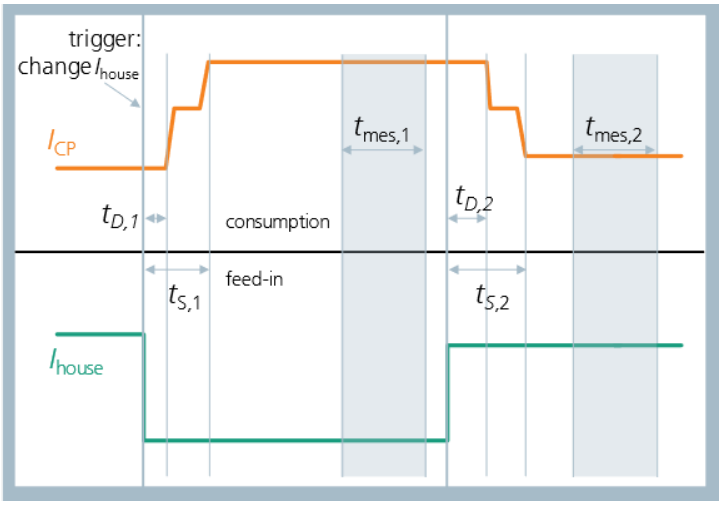

Figure 4: Test sequence of setting current references $-I_{house}$. After a settling time t_S a stable maximum allowed charging current I_{CP} is communicated to the EV.

In order to put a spot on control quality, the following quantities need to be assessed. First, the trigger event, that is the step in I_{house}. Second, the dead time t_D until the first change in the CP signal. Third, the settling time from the trigger event to a steady state t_S. Finally, after a waiting time, I_{CP} is recorded for an interval t_{mes}. During that interval I_{CP} is compared to the expected current $-I_{house}$ and the control deviation $\Delta I_{CP} = I_{house} - I_{CP}$ is calculated.

The described test is repeated for 17 set points of I_{house} for both, single and three phase charging. As different charging scenarios where anticipated the steps sizes range from 0.5 A to 16 A.

3.3 Application Test

The above described procedures determine the system behaviour in an artificial scenario. To observe the systems' behaviour in an application scenario, residual load time series data with 1 s resolution is applied to P_{house}. This data was previously measured in a field system. The ability of the charging systems' set point P_{CP} to follow the reference is quantified through the parameters $E_{feed-in}$ and E_{draw}. $E_{feed-in}$ is the amount of surplus energy that is fed back into the grid, E_{draw} is the amount of energy that has to be drawn from the grid due to control imperfections. Two parameters are chosen to allow for differentiated weighting, as drawing from the grid implicates higher costs. In an optimal scenario, where the controller follows the reference perfectly both parameters would evaluate to zero. In addition, E_{EV}, i.e. the total charged energy to the EV and E_{house}, i.e. the total PV generated energy are calculated. E_{house} should be the same in all test runs, as the same time series data is used, but can vary slightly due to fluctuations in the voltage when current set points are given.

Here, a 5 min section with residual power between 5 kW and 12.5 kW is chosen. It isolates the control steps operational phase for three phase charging with symmetrically loaded phases. This isolation should enable comparability with the parametrization determined in the static control quality scenario.

4 Results

The previously defined test procedures were applied to four different solar charging systems available on the market, named device under test (DUT). The test routines reveal reproducible deviations among the competitors.

4.1 Standby Consumption

As described in section 3.1, the measurement to determine the standby consumptions is conducted over a 30 min time interval for each system state, following the order C, B, A. Figure 5 shows the behaviour of the DUTs in the respective standby state. It is important to note, that the power consumption of the whole DUT as defined in section 2 is measured. That includes, next to the charging station, the energy meter and external EMS where necessary.

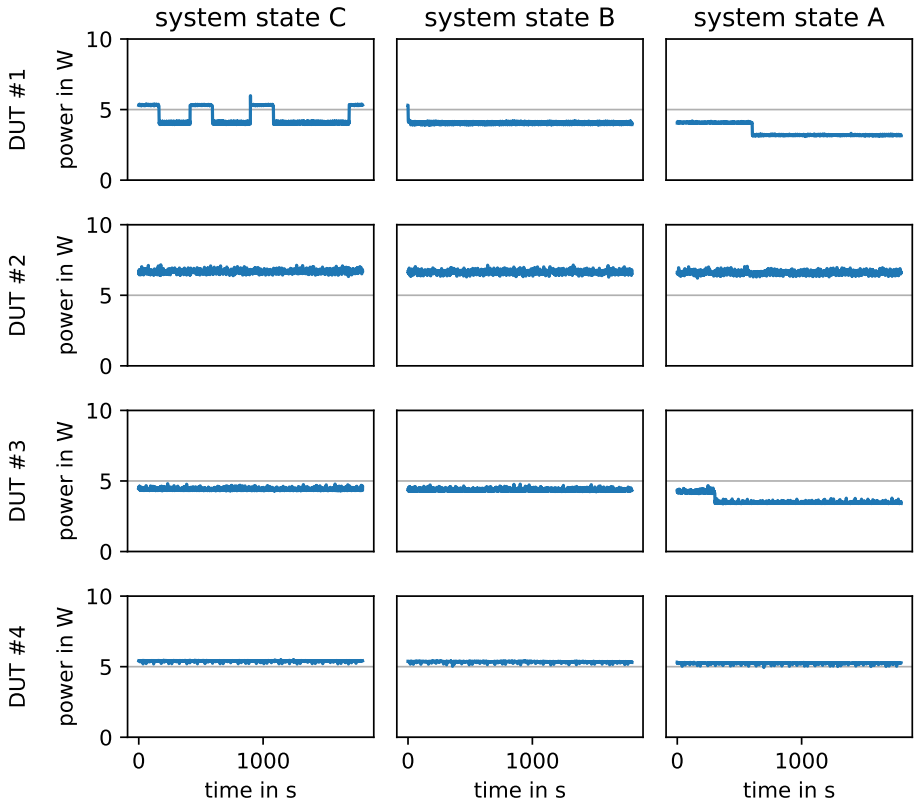

Figure 5: Standby power consumption of the DUTs. In each system state a 30 min interval was captured. The system states were captured consecutively in one run, in the order C (plugged-in, charge request), B (plugged-in, no charge request), A (unplugged).

In each system state, the mean power consumption is calculated over the whole measurement interval. Three of the four devices do not change standby consumption between states C and B. DUT #1 shows alternations in power consumption in state C that can be related to repetitive probing of the CP signal for a response of the connected EV. DUT #1 and DUT #3 show a power drop of about 1 W in state A when the LEDs of the charging station are turned off. In some systems, the switching off of LEDs can be configured by the user and in case of DUT #2 is not set by default. Comparing the devices, in standby state C the mean power consumption ranges from 4.4 W (DUT #3) to 6.6 W (DUT #2), in state B from 4.0 W (DUT #1) to 6.6 W (DUT #2) and in state A from 3.5 W (DUT #1) to 6.6 W (DUT #2).

4.2 Control Quality

For the evaluation of control quality, the measurement was conducted sequentially for the different set points $-I_{house} = [7, 16, 7, 13, 8, 12, 10, 11, 10.5, 11, 10, 12, 8, 13, 7, 16, 7]$ A. In each step, the parameters dead time t_D, settling time t_S and control deviation ΔI_{CP} are derived from the measurement data. On the one hand, this assess the whole power bandwidth of the EVSE. On the other hand, this leads

to different current steps with larger and lower change in current. The measured currents are evaluated according to the description in section 3.2.
Per convention, the default solar charging configurations with current limit 16 A are used for the devices. For better comparability of best case performance, an exception is made for DUT #3 where the control delay is altered from default 90 s to minimum 5 s. DUT #4 does not support phase switching yet, so data is available only for three-phase charging.

Figure 6 shows the behaviour at an exemplary step from $-I_{house} = 16$ A to $-I_{house} = 7$ A. The step in I_{house} triggers the charging stations to adapt the current reference I_{CP}. All show a reaction and stepwise adaption with different characteristics. Some devices react almost instantaneously to the step in I_{house}, while others wait a few seconds before starting the adaption. After settling, DUTs #1, #2, #3 show little to no fluctuations in the settled state, while DUT #4 alternates I_{CP} with an amplitude of about 1 A. DUT #1 has a significant constant offset after settling. In the following, the statistical parameters, calculated over all set points are presented.

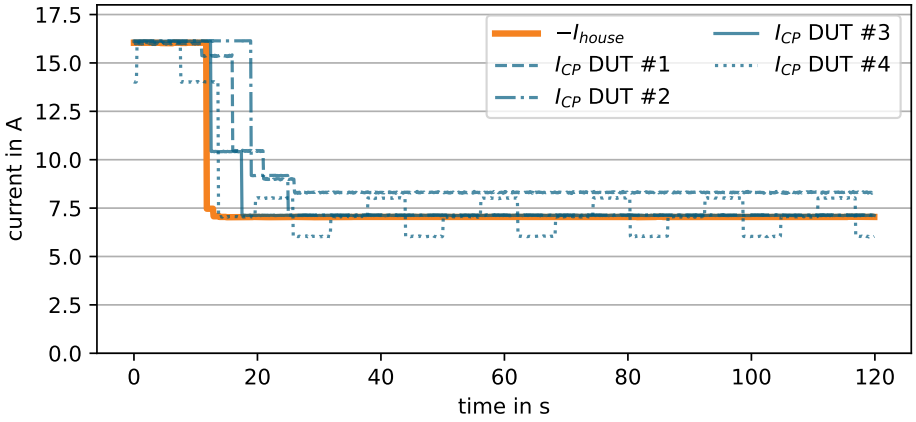

Figure 6: Control behaviour of I_{CP} of the DUTs at an exemplary step. $-I_{house}$ was set from 16 A to 7 A in an active solar charging process.

Figure 7 compares the dead time t_D, i.e. the time between the trigger (step in I_{house}) and the first edge of I_{CP} of the different solar charging systems if available in single and three phase charging mode. Each column in the box plot contains the statistics of t_D over all set points. Comparing the different charging systems and modes, the median dead times vary in the range from 0.9 s (DUT #1) up to 6.3 s (DUT #2), with standard deviations from 1.5 s (DUT #3) up to 3.5 s (DUT #2). Outliers up to 17.4 s correlate with very small steps whose detection generally is worse. Comparing single and three phase charging of a single system, statistics are similar. Single phase charging shows in all three cases smaller median dead times.

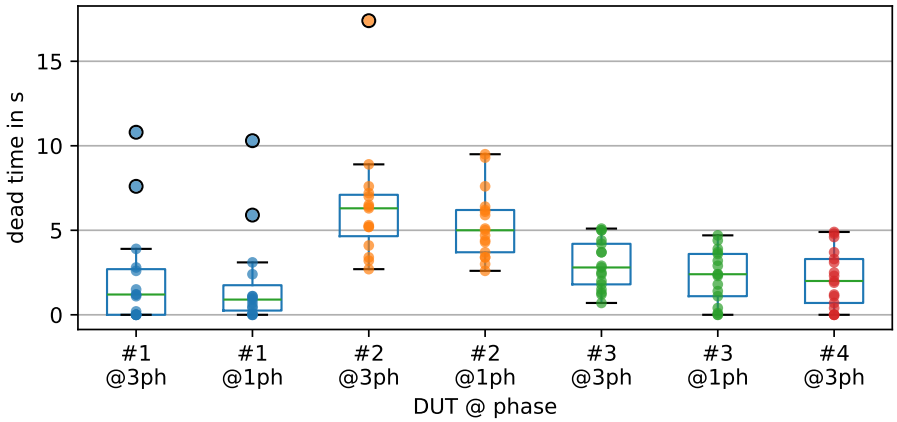

Figure 7: Distribution of the measured dead times t_D in the control quality test for the individual DUTs in three-phase and single-phase charging.

Figure 8 compares the settling time t_S, i.e. the time between trigger (step in I_{house}) and settled I_{CP} (>5 s within range of set point + threshold of 0.5 A) of the different solar charging systems. Each column in the box plot contains the statistics of t_S over all set points. Comparing the different charging systems, the median settling times vary from 4.4 s (DUT #3) up to 16.3 s (DUT #1), with standard deviations from 4.1 s (DUT #2) up to 21.4 s (DUT #3). Outliers up to 72.0 s correlate with larger distances of two consecutive set points. Comparing single and three phase charging of a single system, distributions are similar. Single phase charging shows in all three cases smaller median dead times.

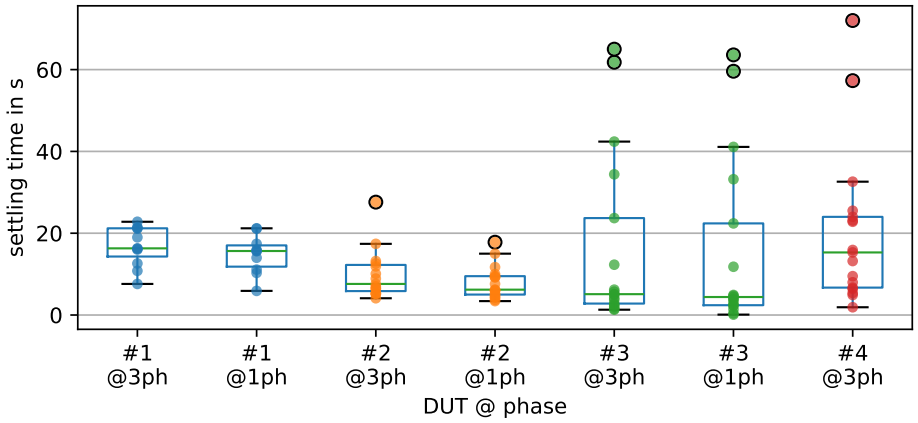

Figure 8: Distribution of the measured settling times t_S in the control quality test for the individual DUTs in three-phase and single-phase charging.

Figure 9 compares the control deviation ΔI_{CP}, i.e. the mean difference between the reference I_{house} and the control signal I_{CP} during a time interval t_{mes} in the steady state of the different solar charging systems. Each column in the box plot contains the statistics of ΔI_{CP} over all set points. Comparing the different charging systems, the median control deviation varies from -0.11 A (DUTs #2, #3) up to -0.43 A (DUT #1), with standard deviations from 0.08 A (DUT #3) up to 0.52 A (DUT #1). Outliers up to 1.27 A correlate with small distances of two consecutive set points and may be explained with measurement inaccuracies and a minimal adaption accuracy of 0.5 A. Comparing single and three phase charging of a single system, distributions are similar.

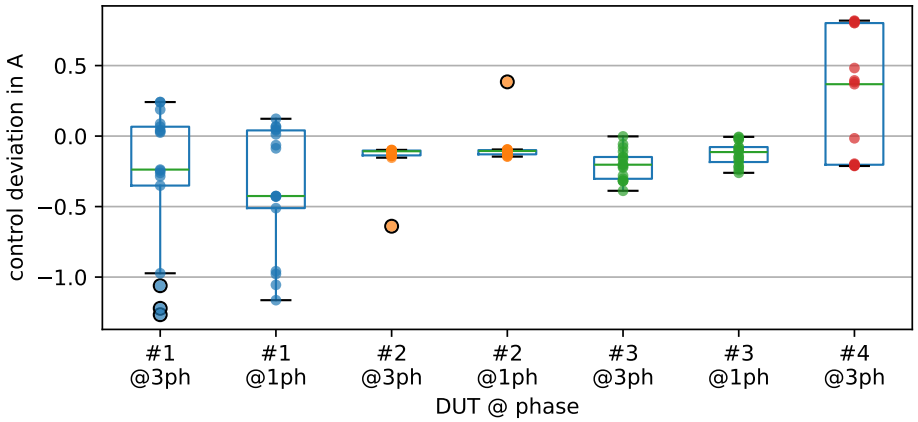

Figure 9: Distribution of the measured control deviations ΔI_{CP} in the control quality test for the individual DUTs in three-phase and single-phase charging.

4.3 Application Test

The 5 min residual load profile described in section 3.3 is applied to the charging systems. Figure 10 shows the different behaviours of P_{CP} when following this reference. The areas where energy is drawn from the grid are marked in grey, the areas where energy is fed into the grid are marked in yellow. It is important to note, that the power limit of the tested systems is 11 kW. Residual power greater than that can not be utilized in the charging process, so $E_{feed-in} = 0$ Wh can not be achieved without curtailment.

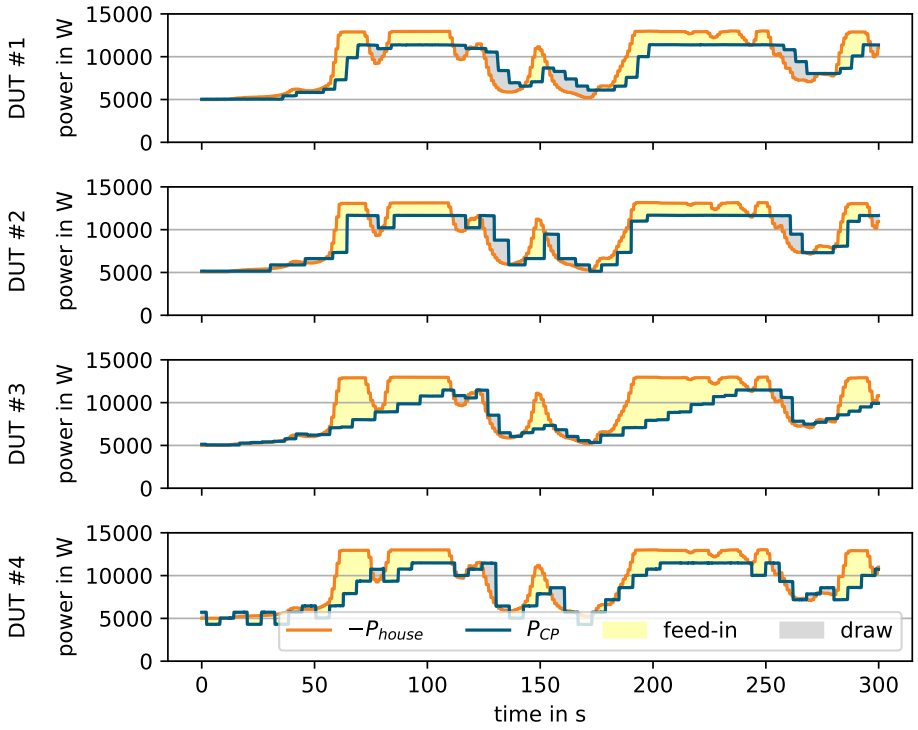

Figure 10: Measurement of dynamic behaviours with a 5 min time series isolated to three phase charging. The phases of the surplus are loaded symmetrically, feed-in and drawn energy is marked.

Table 1 contains the quantities for E_{draw} and $E_{feed-in}$ for the four systems. DUT #1 and #2 demonstrate similar behaviour and an E_{draw} of 50.1 Wh and 49.8 Wh. DUT #3 draws with 17.6 Wh significantly less energy while the feed-in is comparatively higher with 135 Wh vs. 94.7 Wh and 81.1 Wh. This can be explained observing the behaviour of DUT #3 in fig. 10. Ascending control steps of P_{CP} are longer and smaller compared to faster and larger steps when descending. Similar can be observed for DUT #4 as descending steps tend to be of larger amplitude than ascending ones. The asymmetry is not as pronounced as for DUT #3, which also reflects in $E_{draw} = 37.8$ Wh and $E_{feed-in} = 116.1$ Wh, that both lie between the values of DUT #3 and DUTs #1, #2. E_{house} shows variations due to variations of the voltage when the same time series of I_{house} is applied. E_{EV} is the total charged energy.

Table 1: Draw and feed-in energy in the 5 min time series measurement.

	DUT #1	DUT #2	DUT #3	DUT #4
E_{draw} [Wh]	50.1	49.8	17.6	37.8
$E_{feed\text{-}in}$ [Wh]	94.7	81.1	135.0	116.1
E_{EV} [Wh]	740.5	752.0	673.3	704.2
E_{house} [Wh]	789.0	798.1	787.0	790.6

5 Conclusion

For the measurements of both, standby consumption and control quality, reproducible results could be obtained by applying the test routines specified in section 3 to different charging systems available on the market. Table 2 gives an overview of the derived parameters for the respective operational phase.

Standby consumption of the complete systems consisting of charging station, energy meter and (integrated) EMS lies around 5±1.6 W for all tested systems. Two systems show the same standby consumption in all system states, regardless of the EV being connected or not. Two systems exhibit a drop in standby consumption as LEDs are automatically turned off in the disconnected state. One of these also shows fluctuations in the standby consumption when the EV requests charging. This can be related to probing of the CP signal.

Also, the response of the systems when applying time series data from field measurements could be observed under laboratory conditions. The draw and feed-in energy to the grid were determined for a 5 min time series isolating the control steps operational phase and are listed in table 2. Two devices (DUTs #1, #2) show similar results with approximately symmetric ascending and descending behaviour. DUT #3 trades off a higher feed-in for a significantly lower draw by following an asymmetric strategy, i.e. faster descend and slower ascend. DUT #4 shows a similar trade-off but less pronounced.

Table 2: Overview of the derived parameter values from the static test cases and the results from the time series measurement. (feed-in tariff: $8\frac{ct}{kWh}$, electricity price: $30\frac{ct}{kWh}$)

	DUT #1	DUT #2	DUT #3	DUT #4
Standby				
$\bar{P}_{standby,C}$ [W]	4.5 ± 0.60	6.6 ± 0.12	4.4 ± 0.08	5.4 ± 0.03
$\bar{P}_{standby,B}$ [W]	4.0 ± 0.08	6.6 ± 0.12	4.4 ± 0.08	5.4 ± 0.03
$\bar{P}_{standby,A}$ [W]	3.5 ± 0.42	6.6 ± 0.12	3.6 ± 0.29	5.3 ± 0.03
Control Quality				
$\tilde{t}_{D,3ph}$ [s]	1.2 ± 3.1	6.3 ± 3.5	2.8 ± 1.5	2.0 ± 1.7
$\tilde{t}_{D,1ph}$ [s]	0.9 ± 2.8	5.0 ± 2.0	2.4 ± 1.6	n.a.
$\tilde{t}_{S,3ph}$ [s]	16.3 ± 4.9	7.6 ± 6.2	5.1 ± 21.4	15.3 ± 19.0
$\tilde{t}_{S,1ph}$ [s]	15.7 ± 4.8	6.2 ± 4.1	4.4 ± 21.0	n.a.
$\tilde{\Delta I}_{CP,3ph}$ [A]	-0.24 ±0.52	-0.11 ± 0.13	-0.20 ± 0.11	0.37 ± 0.45
$\tilde{\Delta I}_{CP,1ph}$ [A]	-0.43 ±0.44	-0.11 ± 0.12	-0.11 ± 0.08	n.a.
Application Test				
E_{draw} [Wh]	50.1	49.8	17.6	37.8
$E_{feed\text{-}in}$ [Wh]	94.7	81.1	135.0	116.1
electricity cost [ct]	0.75	0.85	-0.55	0.20

The time seriees behaviours can be correlated with the results from the static control quality measurement, especially the derived settling time t_S. Both, DUT #1 and #2 exhibit similar distributions of t_S with little spread compared to DUTs #3, #4 that relates with the symmetric behaviour. DUT #2 has the lowest mean settling time with comparatively little spread and achieves the lowest feed-in. The comparatively high spread of t_S of systems #3 and #4 relates to the assymetric control strategy, i.e. faster adaption for descending steps compared to slower adaption for ascending steps.
The symmetric and the more asymmetric control strategies are two sides of a trade-off. The former risks a higher portion of grid drawn energy for a higher self-consumption, the latter accepts lower self-consumption for less grid supply. To illustrate this: Only considering the solar share on the EV supply would make the DUT #3 1^{st}. But #3 charged less energy to the EV than the other DUTs.

To evaluate which approach is more reasonable one has to consider the grid supply and feed-in tariffs as well as the dimensioning of the PV system. The exemplary electricity cost in table 2 of the five minute application test is derived by multiplying the energy $E_{feed-in}$ by a feed-in tariff of $8\frac{ct}{kWh}$ and E_{draw} with an electricity price of $30\frac{ct}{kWh}$.

It can be stated that standby consumption and the different parameters of control quality, as well as the use case strategies vary significantly among the tested systems. However, it is important to note that some systems offer the possibility to user define system configurations like setting a control delay between 5 s and 180 s or choosing to switch off LEDs in standby mode. These user configurations can have higher impact on the performance than the deviations between different systems with reasonable choice of configurations. This is demonstrated in fig. 11, where the same device with different parametrizations follows the time series from section 3.3.

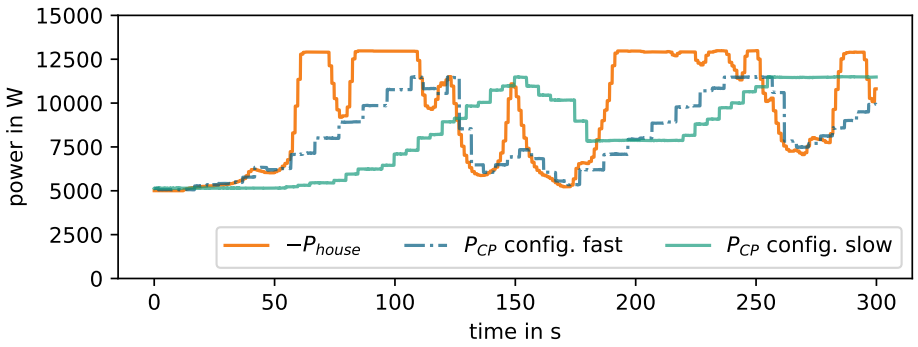

Figure 11: Contrasting behaviour of DUT #3 with two different configurations. In config. fast the user defined delay is set to 5 s, in config. slow it is set to 90 s (default).

Acknowledgments

The work in this contribution has been supported in project “WBInspektion” funded by the German Federal Ministry for Economic Affairs and Climate in the funding scheme “Elektro Mobil” (FKZ: 01MV23027).

References

[1] H. Martin, R. Buffat, D. Bucher, J. Hamper, and M. Raubal, “Using rooftop photovoltaic generation to cover individual electric vehicle demand—a detailed case study,” *Renewable and Sustainable Energy Reviews*, vol. 157, 2022. [Online]. Available: https://doi.org/10.1016/j.rser.2021.111969

[2] VDE, *IEC 61851-1:2017: Electric vehicle conductive charging system - Part 1: General requirements*, https://www.vde-verlag.de/iec-standards/224263/iec-61851-1-2017.html, Std., 2017, vDE-Verlag.

[3] Fraunhofer ISE, “Digital grid lab: Power hardware-in-the-loop laboratory,” http://www.digital-grid-lab.de, accessed: April 2025.

[4] A. N. Morab, S. Marchand, and B. Wille-Haußmann, “Electric vehicle modelling for function testing of charging infrastructures using power hardware-in-the-loop simulations,” in *5th E-Mobility Power System Integration Symposium*, 2021.

[5] F. I. for Solar Energy Systems ISE, “EV Charging Twin toolbox,” 2025, accessed: April 2025. [Online]. Available: https://marketplace.typhoon-hil.com/package?package_name=EV+charging+twin

[6] Typhoon HIL, “Simplify and validate dc fast charging interoperability with hil,” https://www.typhoon-hil.com/webinar/simplify-and-validate-dc-fast-charging-interoperability-with-hil, accessed: April 2025.

[7] Fraunhofer ISE, “Project website: Wallbox-inspektion,” http://www.wallbox-inspektion.de, accessed: April 2025.

Presenter Biography

Dr.-Ing. Bernhard Wille-Haussmann, born in 1977, studied electronic engineering at the University of Stuttgart with focus on communication technologies. Since 2005 he works at Fraunhofer ISE in the field of managing distribution grids with a high penetration of renewable and distributed generators and storages. In June 2011 he finished his PHD with the topic “Usage of the symbolic model reduction for analyzing control strategies in Smart Grids”. Since 2010 he is head of the group Smart Grid Operation and Planning. Since 2021 he is deputy head of the Smart Grid department at Fraunhofer ISE. He is coordinating the work in the Digital Grid Lab (www.digital-grid-lab.de). He offers more than 20 years of experience in the field of smart grids.